

Easy Access to a Family of Polymer Catalysts from Modular Star Polymers

Valentin Rodionov,[‡] Haifeng Gao,[‡] Steven Scroggins, David A. Unruh, Alyssa-Jennifer Avestro, and Jean M. J. Fréchet*

College of Chemistry, University of California, Berkeley, California 94720-1460

Received December 12, 2009; E-mail: frechet@berkeley.edu

Enzymes, Nature's polymer catalysts, are capable of carrying out thousands of competing and often incompatible reactions in a crowded cellular milieu with perfect fidelity and selectivity. These functional linear polyamides create a favorable solvent environment around the catalytic site, isolate it from the action of other enzymes, and are capable of recognizing specific substrates. Enzymes achieve this exquisite level of functionality by folding into intricate tertiary structures.¹

Ab initio rational design of linear polymers capable of protein-like programmed self-assembly remains an elusive goal. Materials with fractal or highly branched topologies are more amenable to molecular engineering due to their globular shape, core-shell microstructure, and multiple functionalization points.² At the same time, these materials can be expected to approximate many of the desirable features of natural biopolymers. Recent publications³ have described the use of branched constructs for the site isolation of catalytic entities and enzyme-like mediation of local solvent environment. In particular, this strategy has allowed our group to combine normally incompatible catalysts in one-pot sequential reaction cascades⁴ without the use of solid supports.⁵

Star polymers, in which several linear polymer chains (arms) are attached to a central core, represent a readily accessed class of branched materials.⁶ These polymers are an attractive target in materials design, since their topological and chemical complexity, which can approach that of dendrimers, is generated in a single key step. To date, few general methods are available for the topologically precise introduction of reactive or catalytic functional groups into star polymers. In the reported syntheses of catalytic star polymers, either the unimolecular core is catalytic⁷ or the catalytic moieties are incorporated via functional monomers in an arm-first process.^{4,8} The unimolecular core approach yields materials with just a few arms, which limits the degree of core isolation and shielding of the local environment.⁹ Furthermore, the functional diversity of the resulting materials is limited, and only a single catalytic moiety is incorporated into each macromolecule. The arm-first polymerization strategy provides access to polymers bearing a wide range of functional groups. However, the morphology of the materials prepared by this process is significantly influenced by the nature of the functional groups being incorporated. A more rapid and general route to star polymers with tunable functionalities and a controlled microstructure is desired. Here we describe the coupling-onto synthesis of star polymers with "clickable"¹⁰ cores. The highly efficient and tolerant copper(I) catalyzed alkyne-azide cycloaddition (CuAAC) reaction¹¹ allowed us to incorporate a wide range of functionalities into the resulting materials. A related approach for incorporation of functionalities into dendrimers via alkene metathesis has been reported recently by our group.¹²

Microemulsion polymerization of styrene, divinylbenzene, and 4-azidomethylstyrene **1** yielded functionalized polystyrene nano-

particles PS(N₃) **2** with a narrow size distribution (Figure 1A). The size of the particles could be controlled between 15 and 50 nm through variations in the ratio of polymerization mixture to surfactant. After purification by precipitation, **2** was reacted with propargylated poly(ethylene glycol) (PEG-alkyne, $M_n \approx 5$ kg/mol) under standard CuAAC conditions as described by Meldal et al.^{11c} Reaction progress was monitored by the disappearance of the characteristic azide band (2097 cm⁻¹) in the IR spectrum of the polymer. The resulting star polymers, (PS(N₃))-PEG **3**, were fully dispersible in water.

We found that the ratio of divinylbenzene cross-linker to monomers used in the microemulsion polymerization step had a profound effect on the reactivity of PS(N₃) nanoparticles. When 2.5 wt % or less of divinylbenzene was added, all of the core azide groups were capable of reacting with the PEG-alkyne. Some azide groups could be left unreacted by purposely using a substoichiometric amount of PEG-alkyne during reaction with PS(N₃). However, subsequent functionalization with polar (**8**, **10**) or highly hydrophobic (**5**, **7**) alkyne payloads (Figure 2B) resulted in materials that formed intractable aggregates in water. When the ratio of divinylbenzene in the polymerization mixture was increased to 5 wt %, only one-third of the azide groups in the cores of the resulting nanoparticles were consumed after a prolonged (96 h) reaction with excess PEG-alkyne, indicating that not all azide groups in the PS(N₃) core were accessible to the relatively large linear PEG chains. Fortunately, smaller molecules do not share this limitation and, following installation of the PEG arms, a wide variety of lower molecular weight payloads were successfully incorporated into the core of (PS(N₃))-PEG via reaction with the remaining azide groups (Figure 2). None of the resulting materials possessed the characteristic signal of the N₃ group in their IR spectra, and their dispersibility in water was unaffected by either hydrophobic or highly polar payloads. The amount of reactive azide groups was determined to be 0.18 mmol/g by measuring the UV absorbance of (PS(N₃))-PEG functionalized with pyrene derivative **4**. We used a feed ratio of 5 wt % of divinylbenzene for synthesizing all of the PS(N₃) nanoparticles in this study.

Dynamic light scattering (DLS) analysis indicated that the hydrodynamic diameter of particles increased from 20 nm to *ca.* 70 nm after PEG-alkyne coupling (Figure 1B). The size of polymer particles observed in the atomic force microscopy (AFM) phase image (Figure 1C) agrees well with the DLS data. The phase image reveals nanoscale material contrast between the cores of the particles and their outer regions. When overlaid, the line profiles of the AFM topography and phase images show a 20–25 nm central core that comprises much of the significant height of the polymer (see Supporting Information). The core appears to be surrounded by a *ca.* 10 nm band of material. The same architecture with well-defined corona and core regions was observed in a transmission electron microscopy image of (PS(N₃))-PEG stained with sodium phosphotungstate (Figure 1D).

[‡] These authors contributed equally.

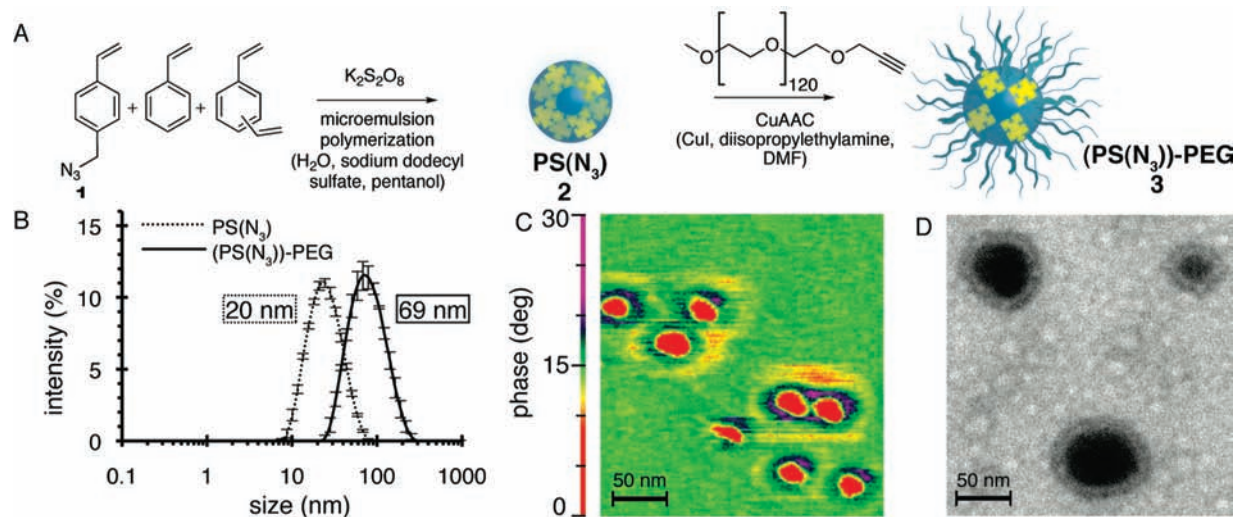


Figure 1. Synthesis and characterization of (PS(N₃))-PEG star polymer **3**. (A) Synthesis of (PS(N₃))-PEG. (B) DLS data for PS(N₃) and (PS(N₃))-PEG in water. (C) AFM phase image of (PS(N₃))-PEG. (D) TEM image of (PS(N₃))-PEG stained with sodium phosphotungstate.

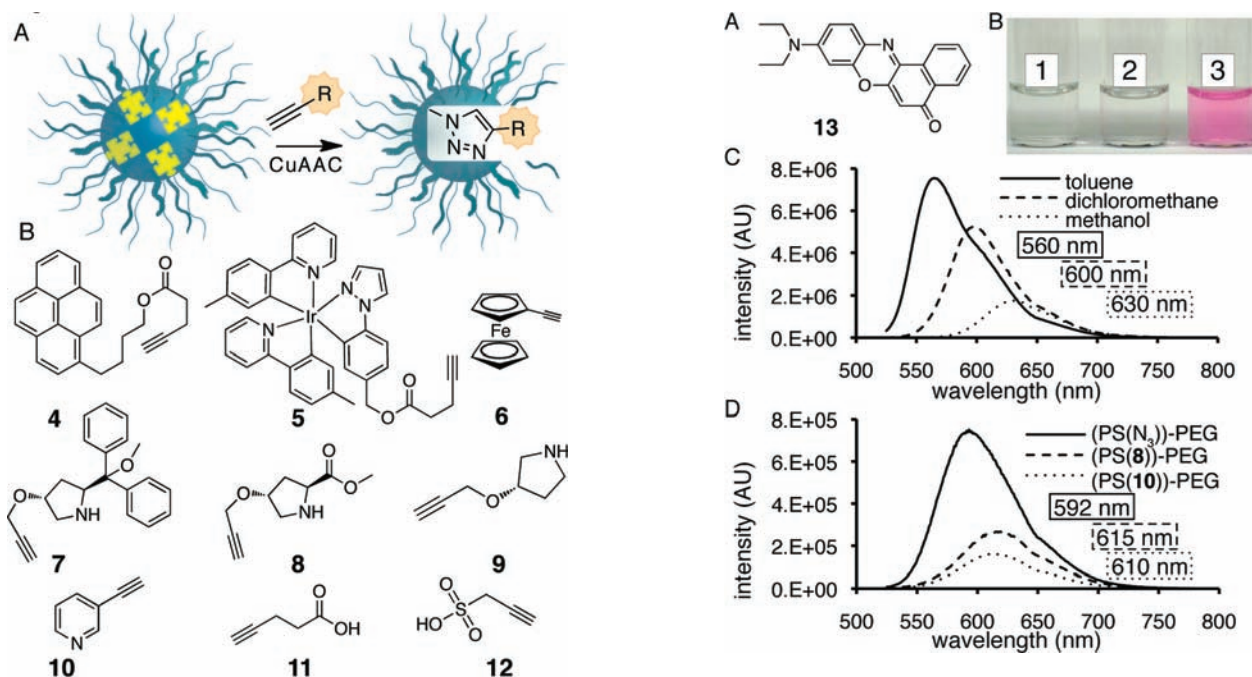


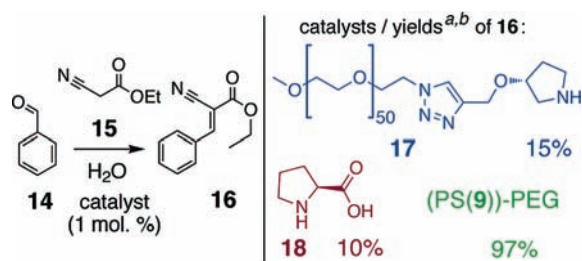
Figure 2. Functional payloads incorporated into (PS(N₃))-PEG star polymers. (A) Coupling of functional alkyne payloads to (PS(N₃))-PEG. (B) Alkynes that were successfully incorporated into (PS(N₃))-PEG. For convenience, the functionalized stars are designated by an abbreviation (PS(X))-PEG, where X is the number of the alkyne payload.

We envision the use of (PS(N₃))-PEG **3** as a water-soluble support for hydrophobic or water-incompatible catalysts. We examined the ability of **3** and its derivatives to transport hydrophobic materials by using Nile Red **13** (Figure 3A), a hydrophobic solvatochromic dye.¹³ Nile Red has a very low solubility in water (Figure 3B, vial 1). The solubility of Nile Red was unaffected by adding 1 wt % of linear PEG ($M_n \approx 5000$ kg/mol) to the solution (Figure 3B, vial 2). In contrast, (PS(N₃))-PEG **3** (1 wt %) was able to efficiently solubilize Nile Red (Figure 3B, vial 3) affording a solution that exhibited a strong emission at $\lambda_{\max} = 592$ nm ($\lambda_{\text{exc}} = 515$ nm), suggesting that the environment of the core had a remarkably low polarity comparable to that of dichloromethane (Figure 3C, 3D). Incorporation of polar heterocyclic cargos such

Figure 3. Fluorescence experiments with solvatochromic dye Nile Red **13**. (A) Nile Red **13**. (B) Transport of **13**: vial 1 contains **13** in water; vial 2 contains **13** in 1 wt % aqueous solution of linear PEG ($M_n \approx 5$ kg/mol); vial 3 contains **13** in 1 wt % aqueous solution of (PS(N₃))-PEG. (C) Fluorescence emission spectra of **13** in toluene, dichloromethane, and methanol ($\lambda_{\text{exc}} = 515$ nm). (D) Fluorescence emission spectra of **13** solubilized in water by (PS(N₃))-PEG, (PS(8))-PEG, and (PS(10))-PEG ($\lambda_{\text{exc}} = 515$ nm).

as ethynylated proline **8**, or pyridine **10**, into the star core resulted in a red shift of the emission wavelength of Nile Red to $\lambda_{\max} = 615$ nm, suggesting a polarity comparable to that of methanol.

To probe the viability of our material as a catalyst support, we used a model Knoevenagel condensation between benzaldehyde **14** and ethyl cyanoacetate **15** in water (Scheme 1). The rate of the uncatalyzed reaction is negligible at room temperature. (PS(9))-PEG demonstrated activity superior to that of L-proline **18**, or the functional PEG **17**. (PS(9))-PEG could be recycled multiple times with no loss of activity (see Supporting Information). We suggest that the superior catalytic activity of our material is due to the

Scheme 1. Model Knoevenagel condensation^{a,b}

^a Reactions were run for 24 h at 20 ± 2 °C in H₂O, [14] = [15] = 0.94 M. ^b Yields are based on GC-MS measurements.

Table 1. Catalytic Results for a One-Pot Reaction Cascade Using Acid and Amine Catalysts^a

Entry	Amine catalyst	Acid catalyst	Conversion of 19 [%] ^c	Yield of 16 [%] ^c
1	pyrrolidine	PTSA	0	0
2	(PS(9))-PEG	PTSA	0	0
3	pyrrolidine	(PS(12))-PEG	0	0
4	(PS(9))-PEG	(PS(12))-PEG ^b	100	95

^a Reactions were run for 24 h at 20 ± 2 °C in H₂O/methanol (4:1), [19] = 60 mM, [15] = 440 mM. 10 mol % of amine and acid catalysts (relative to 19) were used. ^b Loading of ca. 2 mol % of (PS(12))-PEG and 10 mol % of (PS(9))-PEG results in 85% yield of 16 after 3 h, indicating that the star acid is not inactivated even by a large excess of amine star. ^c Yields are based on GC-MS measurements.

placement of catalytic amine moieties within the hydrophobic environment of the core.¹⁴

We used the one-pot cascade transformation of benzaldehyde dimethyl acetal 19 into the Knoevenagel condensation product 16 to evaluate the utility of the new materials for site isolation applications (Table 1).^{4b} We chose (PS(9))-PEG as the amine catalyst for the Knoevenagel condensation step of the cascade and star acid (PS(12))-PEG for the acetal hydrolysis step. Control reactions with *p*-toluenesulfonic acid (PTSA) and pyrrolidine (entry 1), as well as PTSA and (PS(9))-PEG (entry 2) and pyrrolidine and (PS(12))-PEG (entry 3), resulted in no acetal hydrolysis and no cascade product 16 being formed. Complete and rapid conversion of acetal 14 to cascade product 16 was observed for the combination of amine catalyst (PS(9))-PEG with acid star (PS(12))-PEG. These results support our assumption that the star cores are sufficiently isolated from each other to prevent mutual deactivation of incompatible core-bound catalytic groups.

In summary, we have developed a versatile and scalable synthesis of a water-dispersible modular star polymer platform with an enzyme-inspired hydrophobic interior and explored the use of this material for the creation of a local hydrophobic solvent environment in water. We have demonstrated that the core of the materials can be functionalized at will, independently from the modification of the polymer structure. Efforts to employ these “clickable” stars in the synthesis of a library of enzyme-inspired site isolated catalysts that may be used in aqueous medium are underway.

Acknowledgment. We thank Dr. Jill Millstone, Dr. Yonggui Chi, and Dr. Peter Wich for helpful discussions. Financial support of this research by the National Science Foundation (DMR-0906638) is acknowledged with thanks.

Supporting Information Available: Additional experimental details, spectroscopic and analytical data for all new compounds. This material is available free of charge via the Internet at <http://pubs.acs.org>.

References

- (1) Fersht, A. *Structure and Mechanism in Protein Science: A Guide to Enzyme Catalysis and Protein Folding*; W. H. Freeman: New York, NY, 1998.
- (2) (a) Jikei, M.; Kakimoto, M. *Prog. Polym. Sci.* **2001**, *26*, 1233–1285. (b) Kim, Y. *J. Polym. Sci., Part A: Polym. Chem.* **1998**, *36*, 1685–1698. (c) Tomalia, D. A.; Fréchet, J. M. J. *Prog. Polym. Sci.* **2005**, *30*, 217–219. (d) Voit, B. *J. Polym. Sci., Part A: Polym. Chem.* **2000**, *38*, 2505–2525.
- (3) (a) Harth, E. M.; Hecht, S.; Helms, B.; Malmstrom, E. E.; Fréchet, J. M. J.; Hawker, C. J. *J. Am. Chem. Soc.* **2002**, *124*, 3926–3938. (b) Zhao, M.; Helms, B.; Slonkina, E.; Friedle, S.; Lee, D.; DuBois, J.; Hedman, B.; Hodgson, K. O.; Fréchet, J. M. J.; Lippard, S. J. *J. Am. Chem. Soc.* **2008**, *130*, 4352–4363. (c) Hecht, S.; Ihre, H.; Fréchet, J. M. J. *J. Am. Chem. Soc.* **1999**, *121*, 9239–9240. (d) Helms, B.; Liang, C. O.; Hawker, C. J.; Fréchet, J. M. J. *Macromolecules* **2005**, *38*, 5411–5415. (e) Kreiter, R.; Kleij, A. W.; Gebbink, R. J. M. K.; van Koten, G. *Top. Curr. Chem.* **2001**, *217*, 163–199. (f) Diederich, F.; Felber, B. *Proc. Natl. Acad. Sci. U.S.A.* **2002**, *99*, 4778–4781.
- (4) (a) Chi, Y.; Scroggins, S. T.; Fréchet, J. M. J. *J. Am. Chem. Soc.* **2008**, *130*, 6322–6323. (b) Helms, B.; Guillaudeu, S. J.; Xie, Y.; McMurdo, M.; Hawker, C. J.; Fréchet, J. M. J. *Angew. Chem., Int. Ed.* **2005**, *44*, 6384–6387.
- (5) (a) Zeidan, R. K.; Hwang, S. J.; Davis, M. E. *Angew. Chem., Int. Ed.* **2006**, *45*, 6332–6335. (b) Motokura, K.; Fujita, N.; Mori, K.; Mizugaki, T.; Ebitani, K.; Kaneda, K. *J. Am. Chem. Soc.* **2005**, *127*, 9674–9675. (c) Gelman, F.; Blum, J.; Avnir, D. *J. Am. Chem. Soc.* **2002**, *124*, 14460–14463.
- (6) (a) Gao, H.; Matyjaszewski, K. *Prog. Polym. Sci.* **2009**, *34*, 317–350. (b) Hadjichristidis, N.; Pitsikalis, M.; Pispas, S.; Iatrou, H. *Chem. Rev.* **2001**, *101*, 3747–3792.
- (7) Dichtel, W. R.; Baek, K.-Y.; Fréchet, J. M. J.; Rietveld, I. B.; Vinogradov, S. A. *J. Polym. Sci., Part A: Polym. Chem.* **2006**, *44*, 4939–4951.
- (8) Bosman, A. W.; Heumann, A.; Klaerner, G.; Benoit, D.; Fréchet, J. M. J.; Hawker, C. J. *J. Am. Chem. Soc.* **2001**, *123*, 6461–6462.
- (9) Hecht, S.; Vladimirov, N.; Fréchet, J. M. J. *J. Am. Chem. Soc.* **2001**, *123*, 18–25.
- (10) Kolb, H.; Finn, M.; Sharpless, K. *Angew. Chem., Int. Ed.* **2001**, *40*, 2004–2021.
- (11) (a) Meldal, M. *Macromol. Rapid Commun.* **2008**, *29*, 1016–1051. (b) Rostovtsev, V. V.; Green, L. G.; Fokin, V. V.; Sharpless, K. B. *Angew. Chem., Int. Ed.* **2002**, *41*, 2596–2599. (c) Tornøe, C. W.; Christensen, C.; Meldal, M. *J. Org. Chem.* **2002**, *67*, 3057–3062.
- (12) Liang, C. O.; Fréchet, J. M. J. *Macromolecules* **2005**, *38*, 6276–6284.
- (13) (a) Fowler, S. D.; Greenspan, P. *J. Histochem. Cytochem.* **1985**, *33*, 833–836. (b) Greenspan, P.; Fowler, S. D. *J. Lipid Res.* **1985**, *26*, 781–789.
- (14) Font, D.; Jimeno, C.; Pericas, M. *Org. Lett.* **2006**, *8*, 4653–4655.

JA9104842